J Biol Inorg Chem
DOI 10.1007/s00775-010-0682-6

ORIGINAL PAPER

Inhibition and stimulation of formation of the ferroxidase center and the iron core in *Pyrococcus furiosus* ferritin

Kourosh Honarmand Ebrahimi · Peter-Leon Hagedoorn · Wilfred R. Hagen

Received: 17 November 2009 / Accepted: 16 June 2010
© The Author(s) 2010. This article is published with open access at Springerlink.com

Abstract Ferritin is a ubiquitous iron-storage protein that has 24 subunits. Each subunit of ferritins that exhibit high Fe(II) oxidation rates has a diiron binding site, the so-called ferroxidase center (FC). The role of the FC appears to be essential for the iron-oxidation catalysis of ferritins. Studies of the iron oxidation by mammalian, bacterial, and archaeal ferritin have indicated different mechanisms are operative for Fe(II) oxidation, and for inhibition of the Fe(II) oxidation by Zn(II). These differences are presumably related to the variations in the amino acid residues of the FC and/or transport channels. We have used a combination of UV–vis spectroscopy, fluorescence spectroscopy, and isothermal titration calorimetry to study the inhibiting action of Zn(II) ions on the iron-oxidation process by apoferritin and by ferritin aerobically preloaded with 48 Fe(II) per 24-meric protein, and to study a possible role of phosphate in initial iron mineralization by *Pyrococcus furiosus* ferritin (PfFtn). Although the empty FC can accommodate two zinc ions, binding of one zinc ion to the FC suffices to essentially abolish iron-oxidation activity. Zn(II) no longer binds to the FC nor does it inhibit iron core formation once the FC is filled with two Fe(III). Phosphate and vanadate facilitate iron oxidation only after formation of a stable FC, whereupon they become an integral part of the core. These results corroborate our previous proposal that the FC in PfFtn is a stable prosthetic group, and they suggest that its formation is essential for iron-oxidation catalysis by the protein.

K. Honarmand Ebrahimi · P.-L. Hagedoorn · W. R. Hagen (✉)
Department of Biotechnology,
Delft University of Technology,
Julianalaan 67, 2628 BC Delft,
The Netherlands
e-mail: w.r.hagen@tudelft.nl

Keywords Ferritin · Ferroxidase center · Iron oxidation · Isothermal titration calorimetry · Phosphate

Abbreviations

BFR	Heme-containing bacterioferritin from *Escherichia coli*
EcFtnA	*Escherichia coli* ferritin A
FC	Ferroxidase center
HuHF	Human H-chain ferritin
ITC	Isothermal titration calorimetry
MOPS	3-(*N*-Morpholino)propanesulfonic acid
PfFtn	Non-heme ferritin from the hyperthermophilic archaeal anaerobe *Pyrococcus furiosus*

Introduction

Two forms of ferritin have been found in different organisms: mini-ferritin, or Dps (DNA-binding proteins from starved cells), and maxi-ferritin. Mini-ferritin protein appears to occur only in bacteria [1] and archaea [2]. Maxi-ferritin has been found in many forms of life, such as bacteria [3], archaea [4], stramenopiles [5], and vertebrates [6]. Twelve subunits, mini-ferritin, or 24 subunits, maxi-ferritin, assemble to make a hollow spherical protein structure. The function of maxi-ferritin is to oxidize and store iron in a biologically available and nontoxic form [6]. Mini-ferritin can also oxidize and store iron in its cavity [7], and it has been proposed to function in the protection of DNA from reactive oxygen species [8].

In vertebrates, usually two subunits, H, "heavy chain," and L, "light chain," make up the 24-meric ferritin, whereas in bacteria and archaea all 24 subunits are

Published online: 26 June 2010

identical. Three different subunits, H, M, and L chains, have been found in bullfrog ferritin [9], with the catalytic oxidation activity carried by the H and the M subunits. Each subunit of maxi-ferritins that is involved in the fast oxidation of iron has a diiron binding site approximately in the middle of a four α-helix bundle, which is called the ferroxidase center (FC). In contrast, the FC of mini-ferritin is located in the interface between two symmetry-related subunits; the amino acid residues of the two subunits participate in forming the FC [10]. It has been proposed that in mini-ferritins two ferrous ions bind to the FC, and after oxidation they leave the FC to form a core [10]. At least three different mechanisms have been proposed for the function of maxi-ferritins.

Several studies using different techniques, including rapid mixing methods [11–13] and circular dichroism/magnetic circular dichroism spectroscopies [14], have suggested that in mammalian H-chain maxi-ferritin and bullfrog M-chain ferritin, the FC is a so-called substrate active site. Fe(II) is oxidized in the FC and an Fe(III)–O–Fe(III) unit, which is the precursor of the core, is released to the cavity [15–19]. On the basis of a recent paramagnetic-NMR study by Turano et al. [20] using bullfrog M-chain ferritin, it has been proposed that with a transient FC substrate site, the Fe(III)–O–Fe(III) product leaves the FC and passes through a channel system in the protein shell, forming transient clusters of increasing nuclearity, and only after oxidation of an approximately 150–200 Fe(II) per protein does the core formation process start. In contrast, recent EPR [21] and kinetic studies [22] have suggested that the FC of the non-heme ferritin from the hyperthermophilic archaeal anaerobe *Pyrococcus furiosus* (PfFtn) is a stable prosthetic group. We have proposed that after formation of a stable diiron center, Fe(II) on its way to the core is oxidized by the Fe(III) in the FC, and electrons are transferred to another oxidant such as molecular oxygen [22]. A somewhat different mechanism has been proposed for the heme-containing bacterioferritin from *Escherichia coli* (BFR), in which Fe(II) oxidation is catalyzed by a preexisting core with electron transfer to the FC via a specific mononuclear "internal iron" site [23]. This latter mechanism has recently been questioned with the alternative proposal that the FC of bacterioferritin B from *Pseudomonas aeruginosa* acts as a substrate center for oxidation and as a gate for internalization of iron into the protein [24]. In PfFtn and BFR, the presence of a stable FC would likely block passage of Fe(III)–O–Fe(III) units through the protein shell, and therefore the core formation process must be different from that proposed for bullfrog M-chain ferritin by Turano et al. [20]. Thus far, for PfFtn no indication has been obtained for the occurrence of small clusters en route to core formation, and we assume that core formation starts directly after formation of the FC.

The amino acid residues of site A of the FC are conserved among all maxi-ferritins (Fig. 1). Differences in the residues of site B have been observed. For example, in PfFtn, site B has a glutamate, Glu130, which is absent in human H-chain ferritin (HuHF), where it is replaced by an alanine. In bullfrog M-chain ferritin, there is an aspartate, Asp140, in the position corresponding to Glu130 in PfFtn, and BFR has a histidine, His130, here. These variations may be at the origin of different mechanism of iron oxidation by maxi-ferritins.

It has been shown that binding of other metals such as Zn(II) and Tb(III) inhibits the iron-oxidation activity of several ferritins [25–27]. X-ray crystal structures and kinetic studies of iron oxidation have shown that in bacterial ferritin Zn(II) primarily binds to the FC and inhibits the iron-oxidation process [27, 28]. In mammalian ferritin, Zn(II) binds to the threefold channels and to the FC [29–32] and also inhibits iron-oxidation activity. Differences in the residues of the FC and the threefold channel of ferritins appear to be the reason for the observed differences in Zn(II) and Tb(III) binding patterns for mammalian ferritin versus bacterioferritin.

Certain oxoanions, in particular phosphate and vanadate, increase the rate of iron core formation [33]. Ferritins isolated from different sources contain phosphate that is associated with the core in the protein. In bacterial ferritin, the phosphate-to-iron ratio can be as high as close to unity [34, 35]. In contrast, a ratio of approximately 0.1 has been found in mammalian maxi-ferritin [36]. It has been suggested that phosphate has a role in promoting a core surface redox reaction [37] and that phosphate can increase the in vitro oxidation rate of iron by maxi-ferritin [38]. The role of phosphate in iron deposition into maxi-ferritin is not understood. On the basis of Mössbauer spectroscopy it has been suggested that phosphate may increase the oxidation rate of ferrous ion by the FC as a substrate active site in horse spleen ferritin [39]. The findings of other kinetic studies contradict these results and have suggested that phosphate does not affect the initial rate of iron deposition into horse spleen ferritin [40].

In a previous study [22] we presented evidence to suggest that the FC in PfFtn is a stable, catalytically active prosthetic group. In the present work we provide further support for this proposal using Zn(II) binding to PfFtn. We study the binding of Zn(II) to PfFtn and its effect on the initial oxidation rates of apoferritin and of preloaded ferritin, i.e., ferritin in which the 24 FCs have been aerobically preloaded with 48 Fe(II), in the presence and absence of phosphate, and we explore a possible role of phosphate in initial iron mineralization, i.e., formation of a core, by PfFtn.

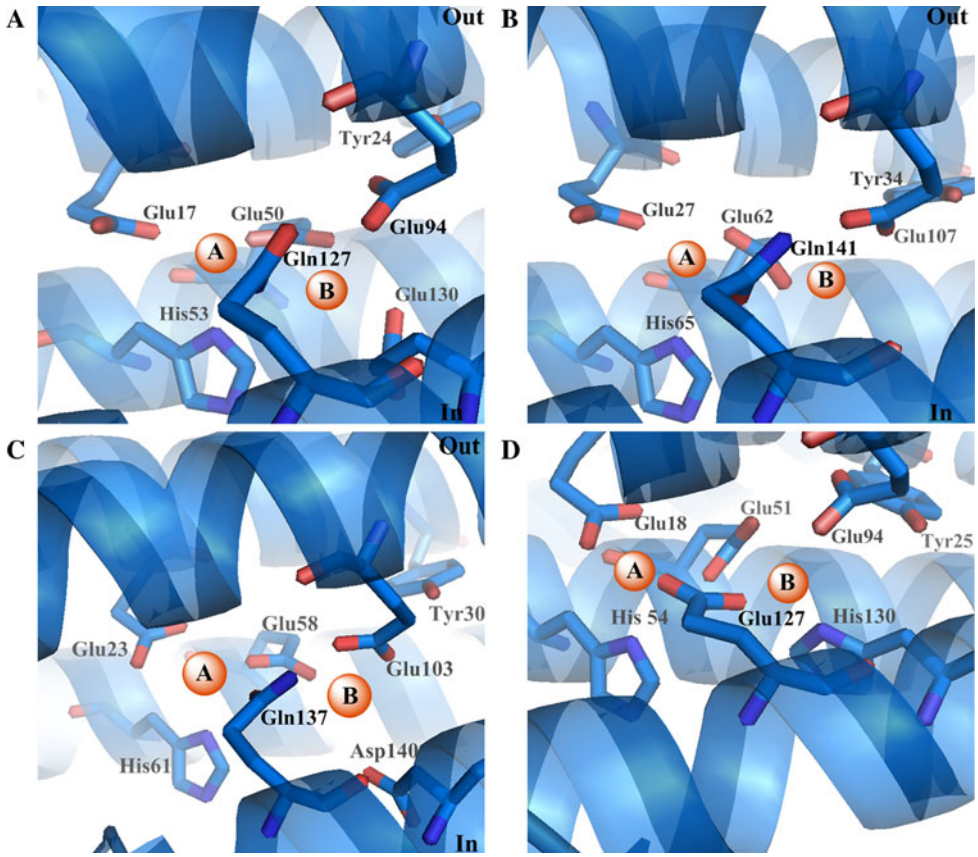

Fig. 1 Structure of the diiron binding site of **a** the *Pyrococcus furiosus* ferritin (PfFtn) [Protein Data Bank (PDB) 2JD7] in comparison with **b** the diiron binding site of human H-chain ferritin (PDB 1FHA), **c** bullfrog M-chain ferritin (PDB 1MFR), and **d** the diiron binding site of *Escherichia coli* bacterioferritin (PDB 3E1J)

Materials and methods

Chemicals

Zinc sulfate was purchased from Merck, anhydrous potassium hydrogen phosphate was from J.T. Baker, and sodium orthovanadate (99.9% metal basis) was from Alfa Aesar. All other chemicals were reagent grade and were purchased from Sigma-Aldrich.

Preparation of apoferritin

PfFtn was expressed and purified as described before [22]. Apoferritin was prepared by the methods of Bauminger et al. [41] and Dawson et al. [42] under anaerobic conditions using nitrogen of 5.0 purity (i.e., 99.999% N_2). The iron content of apoferritin was measured using the ferene method [22]. Apoferritin contains less than one iron per 24-mer. The protein concentration was determined using the bicinchoninic acid assay (Pierce) with bovine serum albumin as a standard.

Kinetics of Fe(II) oxidation

The steady-state kinetics of iron mineralization was followed using a fiber-optic spectrophotometer (Avantes). Progress curves were measured at 315 nm. Spectra were recorded from approximately 5 s after addition of an anaerobic solution of ferrous sulfate. Forty-eight irons per ferritin were added to apoferritin to prepare preloaded samples. Zinc sulfate was used to incubate ferritin with Zn(II) for 10 min. Kinetic measurements were carried out in 100 mM 3-(*N*-morpholino)propanesulfonic acid (MOPS) pH 7.0, using 1-ml glass cuvettes with a path length of 1 cm. The specific activity (defined as micromoles of Fe^{3+} formed per minute per milligram of 24-meric ferritin) was determined from the initial rate measured at 315 nm using an extinction coefficient of 2.5 mM^{-1} cm^{-1} [22]. Three batches of protein were used to measure the kinetics of iron oxidation by apoferritin. Each experiment was performed at least three times with the same or a different concentration of protein. Rapid stopped-flow experiments were carried using a Scientific PQ/SF-53 preparative quench/stopped-flow instrument with an EG&G Princeton Applied Research 1,024-element photodiode-array detector. Measurements were done at 22 °C. Apoferritin mixed with anaerobic water solution was used as a reference sample. Fe(II) oxidation was followed at 315 nm.

Isothermal titration calorimetry measurements

Isothermal titration calorimetry (ITC) experiments of Zn(II) binding to PfFtn were done with a VP-ITC

microcalorimeter (GE Healthcare). All solutions were prepared in the same buffer as the protein, 100 mM MOPS pH 7.0. All solutions were degassed prior to use. Measurements were performed at 25 °C. The experimental parameters for ITC experiments were as follows: reference power 25 μcal s^{-1}, initial delay 100 or 600 s, and stirring speed 307 rpm. The results were analyzed with Origin 7.0. Titration of Zn(II) to the buffer, i.e., in the absence of the protein, was done and the resulting heat of dilution data were subtracted from those of Zn(II) binding to the protein. Each titration was performed twice and the standard deviation of the two independent measurements was determined. The volume of the first injection was 2 μl and the resulting data point was excluded from fits of the integrated heat. The volume of each subsequent injection was 3 μl.

Calorimetry and tryptophan fluorescence

Fluorescence emission spectra were collected during a Zn(II) titration to PfFtn using a Cary spectrofluorimeter at 25 °C. Excitation was done at 295 nm for tryptophan excitation [43, 44]. Measurements were done using quartz cuvettes with a path length of 1 cm. The buffer was 50 mM MOPS pH 7.0. For each titration [four Zn(II) per 24-mer] aliquots of 2 μl aqueous $ZnSO_4$ solution was added to 3 ml protein solution. Approximately 5 min after each addition, the fluorescence spectra were recorded. Longer incubation with Zn(II) did not change the spectra.

Results

Effect of Zn(II) on the fast and slow kinetics of Fe(II) oxidation

It has been shown that Zn(II) decreases the iron-oxidation rate of certain ferritins by binding to the FC [25–31]. To determine the effect of Zn(II) on PfFtn, apoferritin was incubated with various zinc-to-ferritin ratios (i.e., 0–100) for 10 min, and then an aliquot of 48 Fe(II) per ferritin was added to each sample and progress curves were measured at 315 nm. The patterns for apoferritin in the absence of Zn(II) and for apoferritin preincubated with eight and 24 zincs per ferritin are shown in Fig. 2a.

The progress curves show two phases, an initial fast oxidation process followed by a slower oxidation process. The set of progress curves was fitted with a double exponential fit model:

$$A(t) = -M\exp\left(\frac{-t}{T_1}\right) - N\exp\left(\frac{-t}{T_2}\right) + M_0, \qquad (1)$$

where M and N are the pre-exponential amplitude factors and T_1 and T_2 are time constants of the first and the second exponential, respectively. Progress curves were fitted with a global value for T_1, whereas M, N, and T_2 were allowed to differ between traces. The specific activity at time zero was calculated from the first derivative of fits based on Eq. 1. The specific activity for each sample is plotted versus the zinc-to-ferritin ratio in Fig. 2b. It was found that the specific activity of the fast oxidation of Fe(II), attributed to the oxidation of two Fe(II) in the FC, decreases considerably, i.e., up to approximately sevenfold, for preincubated samples with zinc-to-ferritin ratios from 0 to 24. A second, slower reaction is observed for all preincubated samples with zinc-to-ferritin ratios higher than zero (Fig. 2c). The initial rate, N/T_2, of iron oxidation in the second reaction is absent for apoferritin; it starts at a maximum for one zinc per ferritin, and it then continuously decreases with increasing zinc-to-ferritin ratio up to 24. Incubation of PfFtn with 100 Zn(II) per ferritin further decreased the iron-oxidation activity of the FC up to approximately 55-fold.

To determine the stoichiometry of Zn(II) binding to PfFtn and to identify possible additional binding sites, ITC was used. Apoferritin was titrated with zinc as shown in Fig. 3. Two association constants (i.e., two independent binding sites) were required to fit the data. The first site has a higher affinity for Zn(II), $K_1 = (2.4 \pm 0.1) \times 10^4\ M^{-1}$, with a stoichiometry of 1.8 ± 0.1 Zn(II) per subunit. This group of binding sites is presumably the diiron binding site in each of the 24 subunits. The second set of binding sites, with a lower affinity, $K_2 = (6.2 \pm 0.3) \times 10^3\ M^{-1}$, has a stoichiometry of 1.3 ± 0.2 and could be binding to the C site, or acidic residues in the core. The thermodynamic parameters are given in Table 1. Binding of Zn(II) to site A or site B of the FC was marginally resolved: a slightly better fit to the ITC data was obtained with a three sequential binding site model. The results give two similar affinities, $K_1 = (2.5 \pm 0.1) \times 10^4\ M^{-1}$ and $K_2 = (2.2 \pm 0.1) \times 10^4\ M^{-1}$, for binding of Zn(II) to the each site of the FC and a lower affinity, $K_3 = (4.0 \pm 0.1) \times 10^3\ M^{-1}$, for binding to a third site.

Zn(II) binding as a probe for studying the functioning of the FC

To further test our previous proposal [22] that ferric ions are stable in the diiron binding site and do not leave the center, PfFtn was incubated with 24 Zn(II) and 48 Fe(II) per protein in two different orders: (1) incubation of apoferritin with Zn(II) for 10 min and then aerobic incubation of protein with 48 Fe(II) per protein, and (2) aerobic incubation of apoferritin with 48 Fe(II) per protein for approximately 1 h and then 24 Zn(II) per protein for 10 min. An apoferritin sample was incubated with 48 Fe(II) per monomer in the absence of Zn(II) as a control. The

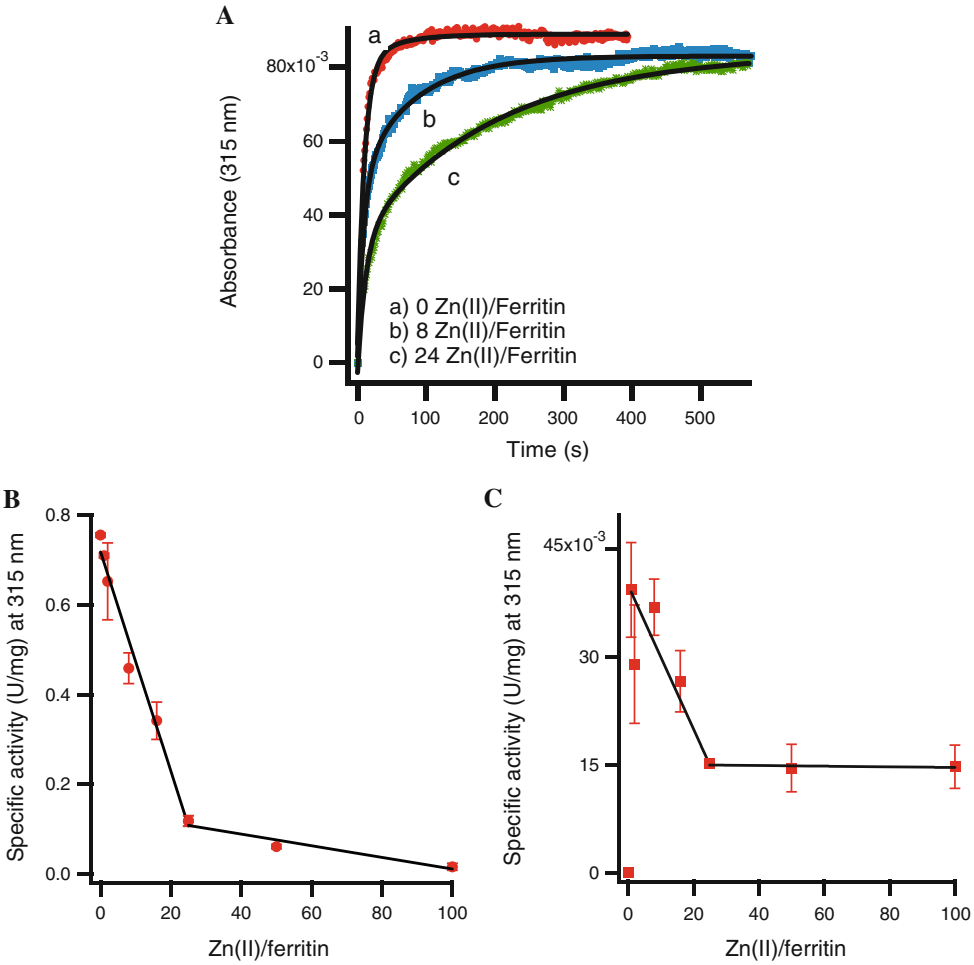

Fig. 2 Effect of Zn(II) on the initial rate of iron oxidation by PfFtn. The concentration of apoferritin was 0.6 μM and measurements were done in 100 mM 3-(*N*-morpholino)propanesulfonic acid (MOPS) pH 7.0 at 25 °C. **a** Progress curves for apoferritin in the absence of Zn(II) (*a*), apoferritin incubated with eight Zn(II) per ferritin (*b*), and apoferritin incubated with 24 Zn(II) per ferritin (*c*). Progress curves were measured at 315 nm. **b** The specific activity of the first oxidation phase attributed to the ferroxidase center (FC) formation versus the Zn(II)-to-ferritin ratio. **c** The specific activity of the slow oxidation phase attributed to the core formation versus the Zn(II)-to-ferritin ratio. The specific activity was calculated using an extinction coefficient of 2.5 cm^{-1} mM^{-1} [21]

progress curve of Fe(III) formation was measured at 315 nm and the results are compared in Fig. 4.

The oxidation rate of 48 Fe(II) added per protein to the sample that was preincubated for 10 min with 24 Zn(II) per protein shows a considerable decrease compared with that of the control sample in the absence of any Zn(II). When apoferritin was incubated with 24 Zn(II) per protein and then incubated with 48 Fe(II) per protein for a longer time, an enhancement in oxidation rate was observed. Apoferritin incubated first with 48 Fe(II) per 24-mer, and then incubated with 24 Zn(II) per protein shows a progress curve similar to that of the control. The minor inhibitory effect of Zn(II) on the 48 Fe(II) per protein preloaded sample does not increase as the time of incubation of the sample with 24 Zn(II) per protein is increased (not shown).

ITC was performed to check the difference between Zn(II) binding to apoferritin and to preloaded ferritin with 48 Fe(II) per ferritin. A preloaded sample was incubated at room temperature at least for 3 h and then at 4 °C for 2 days and then Zn(II) binding to the preloaded sample was measured by ITC (Fig. 5).

Comparing Fig. 5 with Fig. 3, one can see that Zn(II) titration of the iron-preloaded sample [48 Fe(II) per ferritin aerobically] does not show the binding pattern of Zn(II) binding to apoferritin. The results were fitted with a model of two independent binding sites (Table 1). The first site, with higher affinity, $K_1 = (3.1 \pm 1.0) \times 10^4\ M^{-1}$, for Zn(II) has a stoichiometry of less than 0.10 Zn(II) per subunit and the second site, with lower affinity, $K_2 = (3.3 \pm 0.5) \times 10^3\ M^{-1}$, has a stoichiometry of 1.6 ± 0.4 Zn(II) per subunit. Presumably, the substoichiometric strong binding is due to a minor quantity of residual free sites in the more than 95% loaded FCs. Thus, comparing the thermodynamic parameters of Zn(II) binding to the 48 Fe(II) aerobically preloaded sample with that of Zn(II) binding to apoferritin suggests that aerobic addition of 48 Fe(II) per ferritin to apoferritin fills the Zn(II) high-affinity binding sites and Zn(II) is not able to replace iron from these sites. The affinity and thermodynamic parameters of Zn(II) binding to the second set of sites of 48-Fe(II)-preloaded PfFtn are comparable to those for Zn(II) binding to the second set of sites of apo-PfFtn.

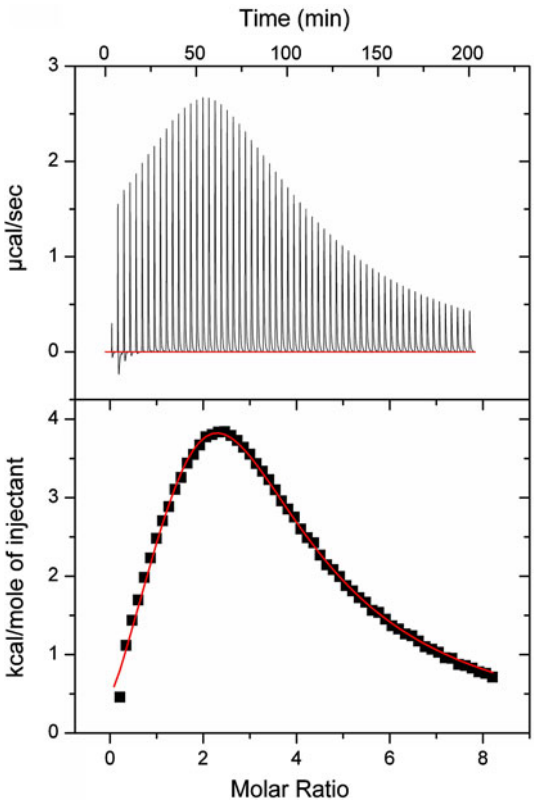

Fig. 3 Binding of zinc to PfFtn. Isothermal titration calorimetry of apoferritin with Zn(II). The concentration of apoferritin in the cell was 4.5 µM (24-mer); the concentration of Zn(II) was 6.5 mM in the syringe. Measurements were done in 100 mM MOPS pH 7.0 and at 25 °C. The ΔH data were fitted to a model with two sets of binding sites. The experimental parameters were as follows: total number of injections 60, volume of each injection 3 µl, duration 6 s, spacing 200 s

Table 1 Theromodynamic parameters for titration of apoferritin and 48 Fe(II) per protein aerobically preloaded *Pyrococcus furiosus* ferritin (*PfFtn*)

Binding parameters	Apo-PfFtn	48 Fe(II)/protein preloaded PfFtn
N_1 per subunit	1.8 ± 0.1	<0.1
K_1 (M^{-1})	(2.4 ± 0.1) × 10^4	(3.1 ± 1.0) × 10^4
ΔH_1 (kcal mol^{-1})	−3.8 ± 0.4	ND
ΔS_1 (cal mol^{-1} $°C^{-1}$)	7.2 ± 1.4	ND
ΔG_1 (kcal mol^{-1})	−6.0 ± 1.5	ND
N_2 per subunit	1.3 ± 0.2	1.6 ± 0.4
K_2 (M^{-1})	(6.2 ± 0.3) × 10^3	(3.3 ± 0.5) × 10^3
ΔH_2 (kcal mol^{-1})	27 ± 4.0	19 ± 2.0
ΔS_2 (cal mol^{-1} $°C^{-1}$)	105 ± 10	82 ± 3.0
ΔG_2 (kcal mol^{-1})	−4.3 ± 1.0	−4.1 ± 1.0

The preloaded sample was incubated at room temperature for at least 3 h and then for 2 days at 4 °C before titration. The concentration of protein (24-mer) was 4.5 µM. The concentration of Zn(II) in the syringe was 6.53 mM. The volume of each injection was 3 µl. The temperature was 25 °C

ND not determined

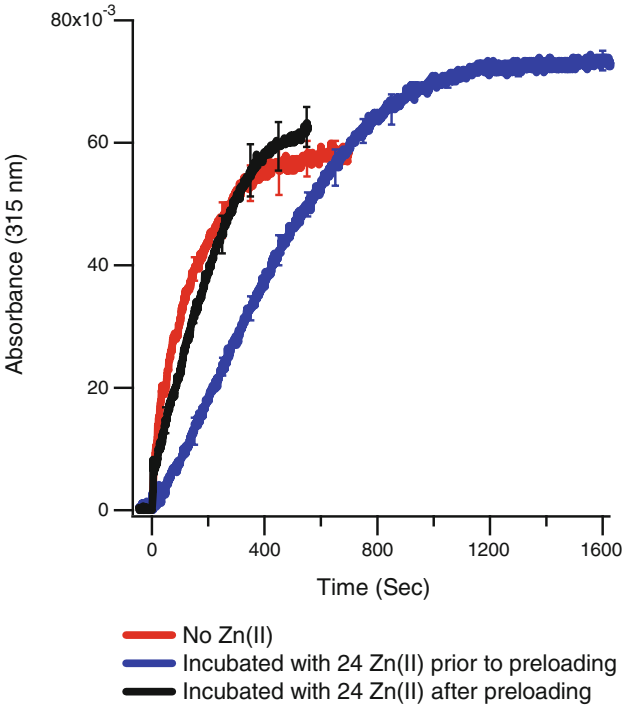

Fig. 4 Inhibitory effect of zinc on iron binding by PfFtn. Progress curves are shown for aerobic addition of 48 Fe(II) per ferritin to a 48-iron-preloaded sample in the absence of Zn(II) (*red*), a preloaded sample that was incubated with 24 Zn(II) per ferritin after preloading (*black*), and a preloaded sample that was incubated with 24 Zn(II) per ferritin prior to preloading (*blue*). The concentration of protein was 0.6 µM and 48 irons per ferritin were added aerobically to preload the apoferritin. The buffer was 100 mM MOPS pH 7.0 and measurements were done at 25 °C

Fluorescence spectroscopy was used to gain more insight into the binding of Zn(II) to apoferritin and 48 Fe(II) per protein aerobically preloaded sample. Excitation at 295 nm was used, which is specific for tryptophan [43]. Two tryptophans are located in the vicinity of the FC: Trp122, which is approximately 10 Å away from site A, and Trp42, which is approximately 10 Å away from site B (Fig. 6a). Both tryptophans are located on the surface of each subunit that faces the cavity of the protein. Addition of Zn(II) increases the fluorescence emission at 324 nm presumably because of conformational changes in the protein [42]. Figure 6b shows that binding of the first 24 Zn(II) per protein clearly differs from that of subsequently added Zn(II). Further additions of Zn(II) increase and shift the fluorescence emission spectra until saturation at approximately 200 Zn(II) per protein.

Analysis of the fluorescence emission spectrum of the 48-Fe(II)-preloaded ferritin showed a different binding pattern of Zn(II) compared with that of apoferritin (Fig. 6c). It can be seen that the slope of the curve of Zn(II) titration to apoferritin at approximately 50 Zn(II) per protein (Fig. 6b) is similar to the initial slope of the curve of Zn(II) titration to the 48 Fe(II)

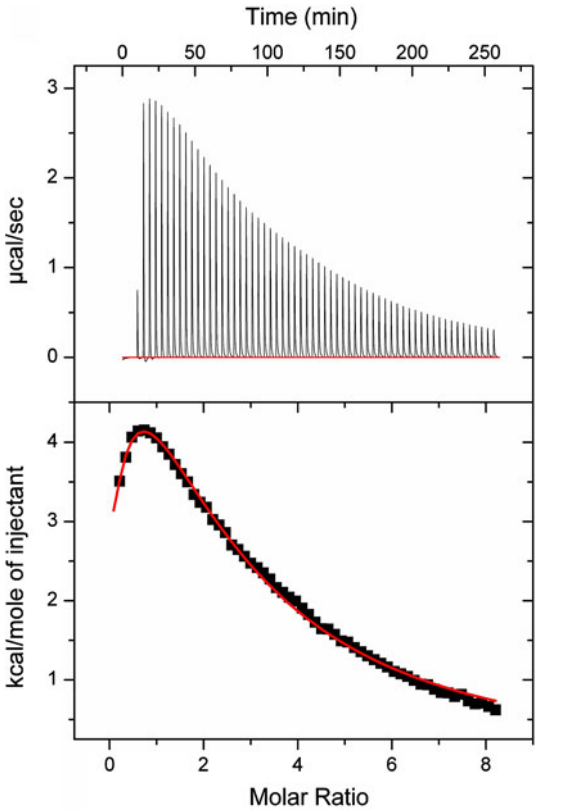

Fig. 5 Effect of iron preloading on the binding of zinc to PfFtn. Isothermal titration calorimetry of a 48 Fe(II) per ferritin preloaded sample with Zn(II). The concentration of ferritin in the cell was 4.5 µM; the concentration of Zn(II) in the syringe was 6.5 mM. The buffer was 100 mM MOPS pH 7.0 and measurements were done at 25 °C. The experimental parameters were as follows: total number of injections 60, volume of each injection 3 µl, duration 6 s, spacing 250 s

per protein preloaded sample (Fig. 6c). Therefore, it appears that the first saturation phase, corresponding to 24 Zn(II) per protein, and part of the second phase, corresponding to 24 Zn(II) per protein, that are observed in binding of Zn(II) to apoferritin have disappeared when apoferritin is preloaded with 48 Fe(II) per protein.

Effect of phosphate on iron oxidation and core formation of PfFtn

Iron was added aerobically to apo-PfFtn in three consecutive steps of 48 Fe(II) per ferritin, in the absence and presence of a ratio of 500 phosphate to ferritin.

From Fig. 7a it can be seen that phosphate does not affect the oxidation rate of the first 48 Fe(II) per ferritin aerobically added to apoferritin; however, it does increase the iron-oxidation rate of subsequent additions of 48 Fe(II) per ferritin by a factor of 6 ± 0.5 (based on measurements with three different batches of protein). The effect of

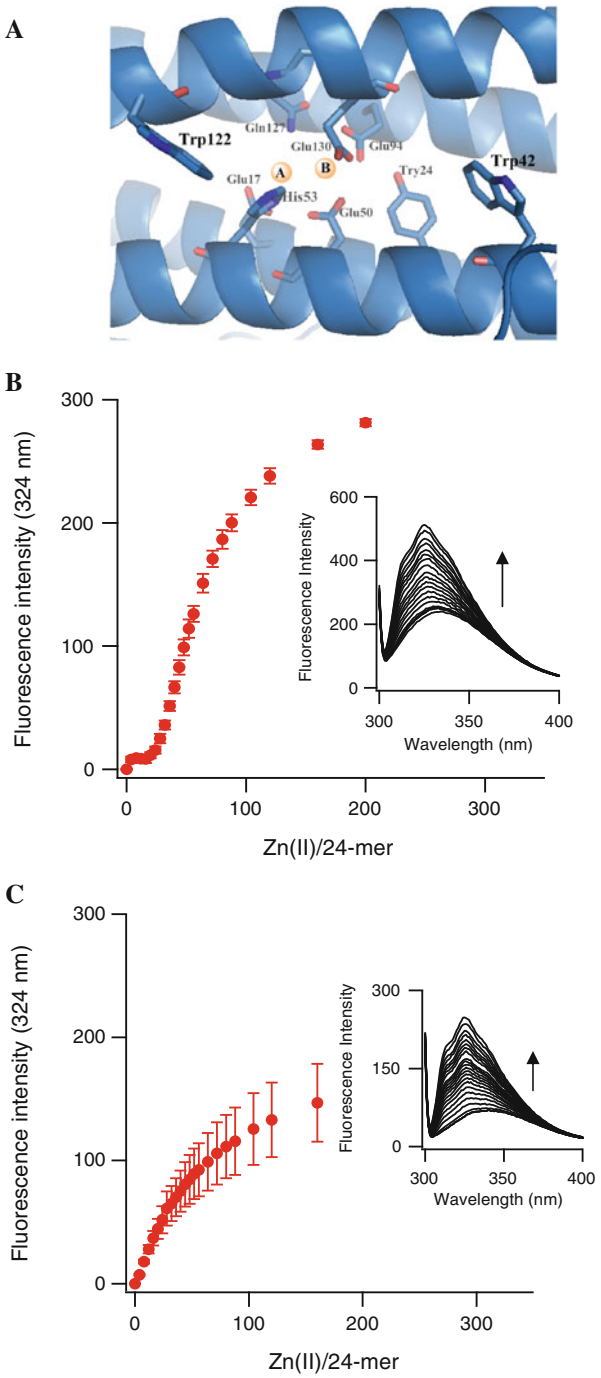

Fig. 6 **a** Structure of the PfFtn subunit with the FC in the middle and two tryptophans, Trp42 and Trp122, each approximately 10 nm away from the FC (PDB 2JD7). **b** Absolute increase (corrected with the spectrum of apoferritin) in fluorescence emission of apoferritin titrated with Zn(II) at 324 nm. The concentration of protein was 0.7 µM. The buffer was MOPS 50 mM pH 7.0. The concentration of aqueous $ZnSO_4$ solution was 4.2 mM. **c** Absolute increase (corrected with the spectrum of the preloaded sample) in fluorescence emission of 48 Fe(II) per protein preloaded ferritin titrated with Zn(II) at 324 nm. The concentration of protein was 0.7 µM and measurements were done in 50 mM MOPS pH 7.0. The concentration of aqueous $ZnSO_4$ solution was 4.2 mM

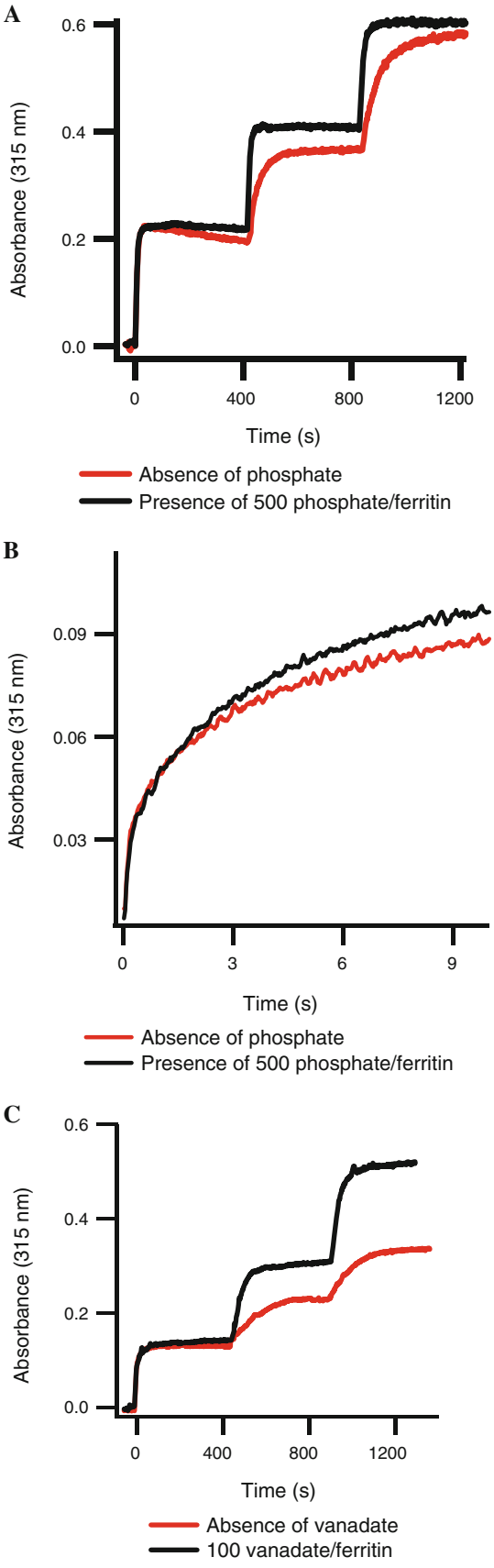

Fig. 7 Stimulatory effect of phosphate and vanadate on the iron-oxidation activity of PfFtn. **a** Three consecutive additions of 48 Fe(II) per ferritin were made in the absence and presence of a phosphate-to-ferritin ratio of 500 (1.65 μM ferritin). **b** Rapid stopped-flow measurements of the initial rate of oxidation of the first 48 Fe(II) per protein by apoferritin in the absence and presence of 500 phosphates per protein. The concentration of protein was 1 μM, and buffer was 400 mM MOPS pH 7.0. Data were collected at 25 °C. The pH of the anaerobic ferrous sulfate solution was 2.5. **c** Three consecutive additions of 48 Fe(II) per ferritin in the absence and presence of 100 vanadates per ferritin (0.825 μM ferritin). Measurements were done in 100 mM MOPS pH 7.0, and at 25 °C

phosphate on the first 48 Fe(II) per protein added to apoferritin was also measured by rapid stopped flow: the data in Fig. 7b confirm the results of the progress curve measurements and show that phosphate does not accelerate the fast oxidation of the first 48 Fe(II) per protein added to apoferritin. It has been shown that not only phosphate but also other oxoanions such as vanadate increase the oxidation rate of iron [38]. Therefore, the effect of vanadate on the iron-oxidation rate of PfFtn was also measured. Fe(II) was again added in three steps of 48 Fe(II) per ferritin, in the presence of a vanadate-to-ferritin ratio of 100. From Fig. 7c it can be seen that the maximum absorbance due to the first addition does not change, whereas vanadate increases the maximum absorbance of the second and the third steps. The effect of phosphate on the initial rates of Fe(II) oxidation was also checked by measuring oxygen uptake rates (data not shown): phosphate does not affect the initial oxygen uptake rate of the first 48 Fe(II) per ferritin added to apoferritin, but it increases the oxidation rate of subsequent additions of the same amount of Fe(II) to PfFtn.

As shown in Fig. 2, when apoferritin is incubated with 24 Zn(II) per ferritin and then 48 Fe(II) per ferritin are added, the oxidation process shows two phases, a fast and a slow one. When this experiment is repeated in the presence of 500 phosphates per ferritin, the oxidation rate of iron in the first process is not changed, but the oxidation rate of the second phase is increased approximately twofold (Fig. 8a).

To test whether functioning of the FC is required for phosphate to increase the oxidation rate of Fe(II), the effect of phosphate was checked when either apoferritin or 48 Fe(II) per ferritin preloaded protein was incubated with 24 Zn(II) per monomer. Again two samples were prepared: (1) apoferritin incubated with 24 Zn(II) per monomer for 10 min and then aerobically incubated with 48 Fe(II) per monomer for approximately1 h, and (2) apoferritin loaded with 48 Fe(II) per monomer and then incubated with 24 Zn(II) per monomer for 10 min. The control was apoferritin incubated aerobically with 48 Fe(II) per ferritin in the absence of any Zn(II). The progress curves were measured for the samples and the control at 315 nm after addition of 48 Fe(II) per protein (Fig. 8b). The results show that the

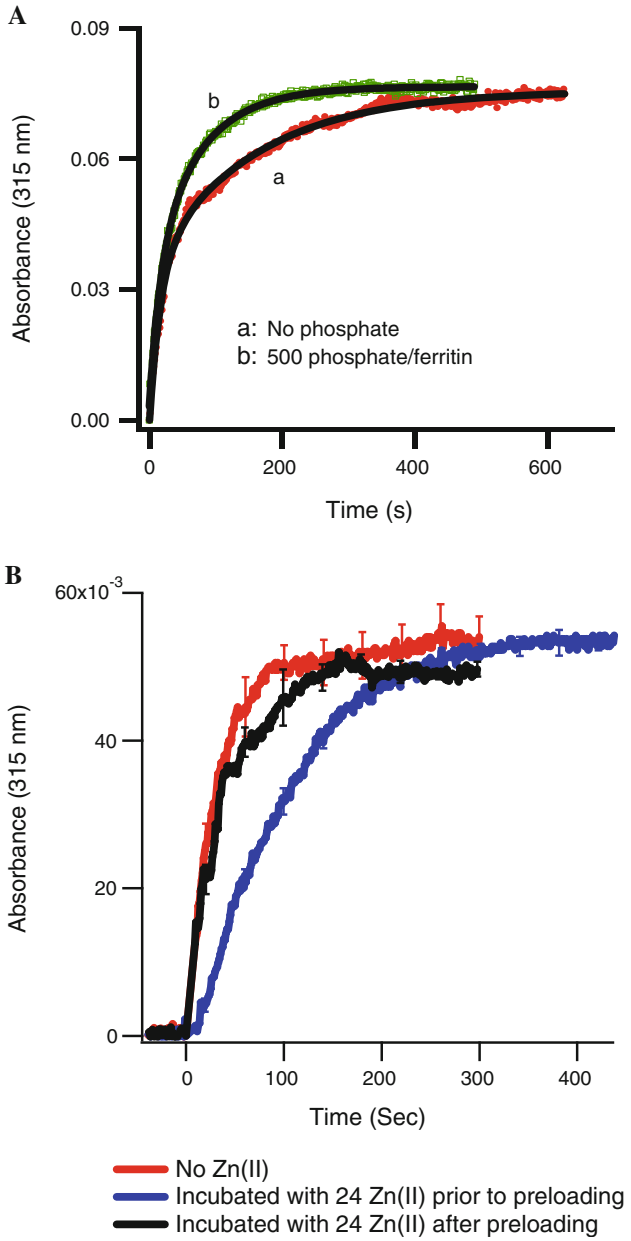

Fig. 8 Effect of zinc on the stimulation by phosphate of the iron-oxidation activity of PfFtn. **a** Forty-eight Fe(II) were added aerobically in the presence or absence of phosphate to apoferritin samples (0.6 μM) that had been preincubated with 24 Zn(II) per ferritin. **b** Forty-eight Fe(II) per ferritin were added aerobically to a PfFtn sample in which the FCs were filled by preloading apoferritin with 48 irons per 24-mer in the absence of Zn(II) (*red*), a PfFtn sample that was aerobically incubated with 48 Fe(II) and subsequently with 24 Zn(II) per ferritin (*black*), and a PfFtn sample that was incubated with 24 Zn(II) and then with 48 Fe per 24-mer (*blue*). The buffer was 100 mM MOPS pH 7.0 and measurements were done at 25 °C

initial oxidation rate for sample 1 is lower than that for the control and that for sample 2. The progress curves for the latter two are identical within experimental error.

To check for phosphate binding to apoferritin or to the Fe(III) in the FC, ITC was used. Titration of phosphate to apoferritin and 48 Fe(II) per ferritin preloaded PfFtn did not show any endothermic or exothermic phosphate binding (not shown).

Discussion

It has been reported that Zn(II) binds to the FC of certain ferritins and inhibits efficient iron oxidation [26–32]. We used the inhibitory effect of Zn(II) to follow the functioning of the FC in iron core formation of PfFtn. To this goal, firstly the inhibiting action of Zn(II) on apo-PfFtn was studied. Apoferritin samples were incubated with Zn(II) in Zn(II)-to-ferritin ratios between 0 and 100. Then 48 Fe(II) per ferritin were added aerobically. Two different processes were observed. The rates of both processes decrease as the amount of Zn(II) increases. It is concluded that 24 Zn(II) per protein, i.e., one Zn(II) per subunit, is enough to impair the functioning of the FC as both the rate of oxidation of Fe(II) in the FC and the rate of core formation decrease. The effect of Zn(II) on the overall core formation reaction suggests that this formation depends on the presence of a stable FC. This observation is in agreement with our previous observation [22] that when an increasing amount of stable FC is formed upon aerobic preloading of apoferritin with different Fe(II)-to-ferritin ratios, the specific activity of the second reaction increases for Fe(II)-to-ferritin preloading ratios of 1–48. Addition of Zn(II) to apoferritin beyond 24 Zn(II) per subunit further decreased the iron-oxidation rate, and at 100 Zn(II) per protein a very slow rate, i.e., 55-fold less than in the absence of zinc, was observed. This slow oxidation of Fe(II) perhaps occurs because of binding of iron to acidic residues in the core and their oxidation by an unknown process. This process may be similar to the slow oxidation and mineralization of iron by the recombinant L ferritin that lacks the FC residues [45]. ITC of apoferritin with Zn(II) shows two independent binding sites, one with a stoichiometry of approximately 2 and relatively higher affinity, consistent with binding of two Zn(II) to the FC, and one with a stoichiometry of approximately 1.3 and lower affinity. Fitting the data with three sequential binding sites suggests that the affinity of binding to one of the FC sites is slightly higher than that for the other site.

Fluorescence spectroscopy of Zn(II) titration of apoferritin shows two phases. Binding of the first 24 Zn(II) per protein causes a minor increase and shift in the fluorescence emission spectra of PfFtn. Since these changes in tryptophan fluorescence typically reflect conformational changes in the protein [46], the data suggest that the first 24 Zn(II) per protein induce only a minor conformational change, possibly because of binding of Zn(II) to site A of the FC with His53 as a ligand to the metal. The observation of two phases for Zn(II) binding to apo-PfFtn differs from

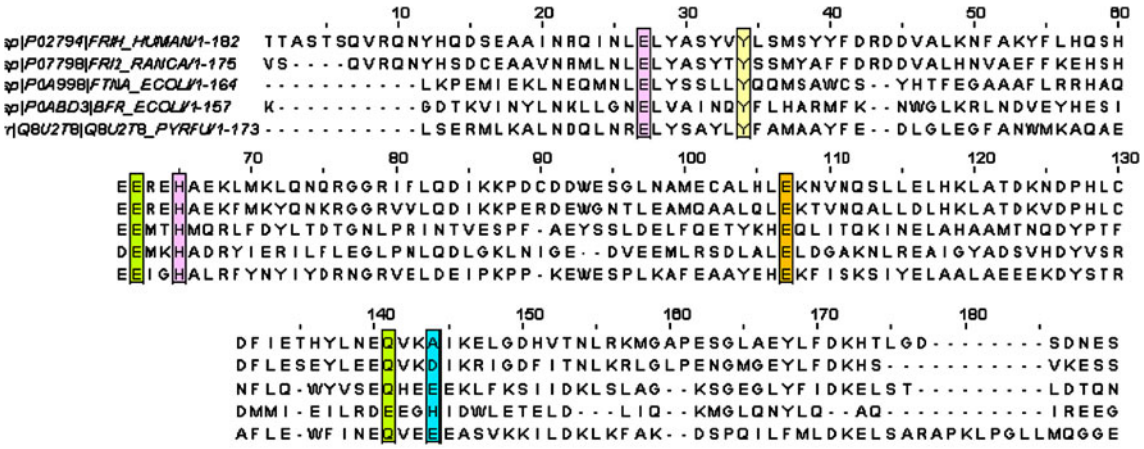

Fig. 9 Amino acid sequence alignment of human H-chain ferritin, bullfrog M-chain ferritin, *E. coli* ferritin A, *E. coli* bacterioferritin, and PfFtn. The residues of site A that are conserved in all ferritins are shown in *pink* and those of site B are shown in *orange*. The residues that are bridging ligands between sites A and B are shown in *green* and the residue of site B that varies among ferritins is shown in *blue*. A conserved tyrosine residue in the vicinity of site B of the FC is shown in *yellow*. The sequence of ferritins was aligned using the T-Coffee tool on the EMBL-EBI server

the results reported for BFR [43]. A possible reason could be the difference in the amino acid residues of the FC between PfFtn and BFR (Fig. 9). Both sites of the FC in BFR have a histidine, His54 and His130, as a ligand. His130 in BFR is replaced by a glutamate, Glu130, in PfFtn. In BFR two glutamates act as bridging ligands between sites A and B, Glu51 and Glu127. In PfFtn only one glutamate, Glu50, acts as the bridging ligand. The second bridging ligand in BFR, Glu127, is replaced with a glutamine, Gln127, in PfFtn. Finally, in PfFtn two tryptophans, Trp122 and Trp42, are located in the vicinity of the PfFtn FC compared with one tryptophan, Trp133, in BFR. The findings that Zn(II) initially fills the FC and has higher affinity for one of the FC sites are similar to results previously reported for *E. coli* ferritin A (EcFtnA) [47]. It has been shown that in EcFtnA, Zn(II) initially fills the FC and it has higher affinity for site A of the FC. Alignment of the amino acid sequences of several ferritins (Fig. 9) shows that PfFtn and EcFtnA have a high degree of identity and the residues of the FC are conserved between them. In comparison, a different Zn(II) binding pattern has been observed for HuHF [29]. On the basis of ITC and the kinetics of iron-oxidation experiments, it has been suggested that in HuHF one Zn(II) binds to the threefold channel, and then other low-affinity sites, including the FC, are filled. Differences between the amino acid residues of the FC and the threefold channel of HuHF versus PfFtn could be the basis for the observed differences in the Zn(II) binding patterns in these two ferritins. The alignment of the two ferritins (Fig. 9) shows that in HuHF there is a cysteine in the threefold channel, which is replaced by Arg117 in PfFtn. Besides, in PfFtn, site B of the FC has a glutamate, Glu130, which is absent in HuHF.

The kinetic measurements in the presence of Zn(II) with apoferritin and preloaded ferritin showed that Zn(II) has an inhibitory effect only when apoferritin is incubated with Zn(II) before preloading with iron. ITC and fluorescence spectroscopy experiments indicated that preloading apoferritin with 48 Fe(II) per ferritin fills the Zn(II) primary binding sites. Because it is known that Fe(II) is primarily oxidized in the FC, the kinetics, fluorescence emission spectra, and ITC results together suggest that Zn(II) primarily binds to the FC. Two conclusions are drawn: (1) the functional model in which Fe(III) is stable in the FC is corroborated because in the alternative "substrate model" zinc would be able to bind following transfer of Fe–O–Fe units from the FC to the core; and (2) formation of a functional FC is essential for further catalytic oxidation of Fe(II), by PfFtn. Alternatively, it may be surmised that Zn(II) binds to other places in the core and then prevents core formation or it may bind to a site in threefold channels and prevent access of Fe(II) to the FC as a substrate site. In both of these alternative scenarios it is expected that Zn(II) binding to apoferritin and to 48 Fe(II) per protein preloaded sample when measured by ITC and fluorescence emission would show similar patterns, which is, however, contradicted by our results.

The role, if any, of phosphate in initial iron mineralization by ferritin is not known. It has been proposed that phosphate binds to the core [33–35] and stimulates the core surface redox reaction [36]. We checked the effect of phosphate and vanadate as an analog of phosphate on the core formation reaction. The results suggest that phosphate and vanadate do not affect the fast oxidation of the first 48 Fe(II) per ferritin added to apoferritin, and are therefore not involved in formation of the FC. Phosphate and vanadate

increase the oxidation rate of Fe(II) only after formation of the FC. The increase in the Fe(II) oxidation rate after FC formation is not significantly different in the presence of phosphate versus vanadate, indicating that the effect is not specific for phosphate. However, the final absorption at 315 nm from the core is approximately twofold higher in the presence of vanadate compared with phosphate, which strongly suggests that the oxoanions actually become part of the core structure only after FC formation.

Finally, it is observed that if the functioning of the FC is impaired by incubating apoferritin with Zn(II), phosphate can no longer increase the oxidation rate. Therefore, although studies by other groups have suggested that phosphate binds to the core and increases the initial iron oxidation [37], our results rather suggest that preformation of the FC and not the core is necessary for phosphate to increase the initial iron-oxidation rate by PfFtn. Furthermore, the phosphate and vanadate experiments once more suggest that oxidation of the first 48 Fe(II) per ferritin proceeds via a mechanism different from that for any subsequent addition of Fe(II). To understand the mechanism(s) by which phosphate increases the oxidation rate of Fe(II) after FC formation, further investigations are required.

Acknowledgments We thank Maurits Peters and Anne Hoekstra for their experimental assistance. This work was supported by a research grant from the Dutch National Research School Combination, Catalysis Controlled by Chemical Design (NRSC-Catalysis).

Open Access This article is distributed under the terms of the Creative Commons Attribution Noncommercial License which permits any noncommercial use, distribution, and reproduction in any medium, provided the original author(s) and source are credited.

References

1. Ilari A, Ceci P, Ferrari D, Rossi GL, Chiancone E (2002) J Biol Chem 277:37619–37623
2. Wiedenheft B, Mosolf J, Willits D, Yeager M, Dryden KA, Young M, Douglas T (2005) Proc Natl Acad Sci USA 102:10551–10556
3. Yariv J, Kalb AJ, Sperling R, Bauminger ER, Cohen SG, Ofer S (1981) Biochem J 197:171–175
4. Matias PM, Tatur J, Carrondo MA, Hagen WR (2005) Acta Crystallogr A 61:503–506
5. Marchetti A, Parker MS, Moccia LP, Lin EO, Arrieta AL, Ribalet F, Murphy MEP, Maldonado MT, Armbrust EV (2009) Nature 457:467–470
6. Liu X, Theil EC (2005) Acc Chem Res 38:167–175
7. Bellapadrona G, Stefanini S, Zamparelli C, Theil EC, Chiancone E (2009) J Biol Chem 284:19101–19109
8. Grant RA, Filman DJ, Finkel SE, Kolter R, Hogle JM (1998) Nat Struct Biol 5:294–303
9. Ha Y, Shi D, Small GW, Theil EC, Allewell NM (1999) J Biol Inorg Chem 4:243–256
10. Kim SG, Bhattacharyya G, Grove A, Lee YH (2006) J Mol Biol 361:105–114
11. Bou-Abdallah F, Zhao G, Mayne HR, Arosio P, Chasteen ND (2005) J Am Chem Soc 127:3885–3893
12. Bou-Abdallah F, Zhao G, Biasiotto G, Poli M, Arosio P, Chasteen ND (2008) J Am Chem Soc 130:17801–17811
13. Tosha T, Hasan MR, Theil EC (2008) Proc Natl Acad Sci USA 105:18182–18187
14. Schwartz JK, Liu XS, Tosha T, Theil EC, Solomon EI (2008) J Am Chem Soc 130:9441–9450
15. Hwang J, Krebs C, Huynh BH, Edmondson DE, Theil EC, Penner-Hahn JE (2000) Science 287:122–125
16. Jameson GNL, Jin W, Krebs C, Perreira AS, Tavares P, Liu X, Theil EC, Huynh BH (2002) Biochemistry 41:13435–13443
17. Liu X, Theil EC (2004) Proc Natl Acad Sci USA 101:8557–8562
18. Waldo GS, Ling J, Sanders-Loehr J, Theil EC (1993) Science 259:796–798
19. Zhao G, Bou-Abdallah F, Arosio P, Levi S, Janus-Chandler C, Chasteen ND (2003) Biochemistry 42:3142–3150
20. Turano P, Lalli D, Felli IC, Theil EC, Bertini I (2010) Proc Natl Acad Sci USA 107:545–550
21. Tatur J, Hagen WR (2005) FEBS Lett 579:4729–4732
22. Honarmand Ebrahimi K, Hagedoorn PL, Jangejon JA, Hagen WR (2009) J Biol Inorg Chem 14:1265–1274
23. Crow A, Lawson TL, Lewin A, Moore GR, Le Brun NE (2009) J Am Chem Soc 131:6808–6813
24. Weeratunga SK, Lovell S, Yao H, Battaile KP, Fischer CJ, Gee CE, Rivera M (2010) Biochemistry 49:1160–1175
25. Le Brun NE, Keech AM, Mauk MR, Mauk AG, Andrews SC, Thomson AJ, Moore GR (1996) FEBS Lett 397:159–163
26. Treffry A, Harrison PM (1984) J Inorg Chem 21:9–20
27. Yang X, Le Brun NE, Thomson AJ, Moore GR, Chasteen ND (2000) Biochemistry 39:4915–4923
28. Stillman TJ, Hempstead PD, Artymiuk PJ, Andrews SC, Hudson AJ, Treffry A, Guest JR, Harrison PM (2001) J Mol Biol 307:587–603
29. Bou-Abdallah F, Arosio P, Levi S, Janus-Chandler C, Chasteen ND (2003) J Biol Inorg Chem 8:489–497
30. Toussaint L, Bertrand L, Hue L, Crichton RR, Declercq JP (2007) J Mol Biol 365:440–452
31. Yablonski MJ, Theil EC (1992) Biochemistry 31:9680–9684
32. Sun S, Arosio P, Levi S, Chasteen ND (1993) Biochemistry 32:9362–9369
33. Johnson JL, Cannon M, Watt RK, Frankel RB, Watt GD (1999) Biochemistry 38:6706–6713
34. Watt GD, Frankel RB, Jacobs D, Huang H, Papaefthymiou GC (1992) Biochemistry 31:5672–5679
35. Rohrer JS, Islam QT, Watt GD, Sayes DE, Theil EC (1990) Biochemistry 29:259–264
36. Treffry A, Harrison PM (1978) Biochem J 171:313–320
37. Proulx-Curry PM, Chasteen ND (1995) Coord Chem Rev 144:347–368
38. Polanams J, Ray AD, Watt RK (2005) Inorg Chem 44:3203–3209
39. Cheng YG, Chasteen ND (1991) Biochemistry 30:2947–2953
40. Sun S, Chasteen ND (1992) J Biol Chem 267:25160–25166
41. Bauminger ER, Harrison PM, Hechel D, Nowik I, Treffry A (1991) Biochim Biophys Acta 1118:45–58
42. Dawson MC, Elliott DC, Elliot WH, Jones KM (1986) Data for biochemical research, 3rd edn. Clarendon Press, Oxford
43. Mely Y, Rocquigny HD, Morellet N, Roques BP, Gerard D (1996) Biochemistry 35:5175–5182
44. Lawson TL, Crow A, Lewin A, Yasmin S, Moore GR, Le Brun NE (2009) Biochemistry 48:9031–9039
45. Levi S, Salfeld J, Franceschinelli F, Cozzi A, Dorner MH, Arosio P (1989) Biochemistry 28:5179–5184
46. Khanna NC, Tokuda M, Waisman DM (1986) J Biol Chem 261:8883–8887
47. Treffry A, Zhao Z, Quail MA, Guest JR, Harrison PM (1998) J Biol Inorg Chem 3:682–688